Journal of Radiation Research, 2013, 54, 578–586
doi: 10.1093/jrr/rrs109 Advance Access Publication 23 November 2012

Determining photon energy absorption parameters for different soil samples

Nil KUCUK[1,*], Zeynal TUMSAVAS[2] and Merve CAKIR[1]

[1]Department of Physics, Faculty of Arts and Sciences, Uludag University, Gorukle Campus, 16059 Bursa, Turkey
[2]Department of Soil Science, Faculty of Agriculture, Uludag University, Gorukle Campus, 16059 Bursa, Turkey
*Corresponding author. Department of Physics, Faculty of Arts and Sciences, Uludag University, Gorukle Campus, 16059 Bursa, Turkey. Tel: + 90-224-294-1705; Fax: + 90-224-294-1899; Email: nilkoc@uludag.edu.tr

(Received 23 July 2012; revised 23 October 2012; accepted 24 October 2012)

The mass attenuation coefficients (μ_s) for five different soil samples were measured at 661.6, 1173.2 and 1332.5 keV photon energies. The soil samples were separately irradiated with ^{137}Cs and ^{60}Co (370 kBq) radioactive point gamma sources. The measurements were made by performing transmission experiments with a 2″ × 2″ NaI(Tl) scintillation detector, which had an energy resolution of 7% at 0.662 MeV for the gamma-rays from the decay of ^{137}Cs. The effective atomic numbers (Z_{eff}) and the effective electron densities (N_{eff}) were determined experimentally and theoretically using the obtained μ_s values for the soil samples. Furthermore, the Z_{eff} and N_{eff} values of the soil samples were computed for the total photon interaction cross-sections using theoretical data over a wide energy region ranging from 1 keV to 15 MeV. The experimental values of the soils were found to be in good agreement with the theoretical values. Sandy loam and sandy clay loam soils demonstrated poor photon energy absorption characteristics. However, clay loam and clay soils had good photon energy absorption characteristics.

Keywords: soil sample; gamma-ray transmission; mass attenuation coefficient; effective atomic number; effective electron density

INTRODUCTION

Soils have chemical composition characterized by the presence of major compounds, such as $Si0_2$, Al_20_3, CaO, Fe_2O_3 and MgO, and have physical properties, including water holding capacity, moistness, particle density, appearance density, porosity, and the concentrations of sand, silt, clay and loam. Soils also contain microelements such as Zn, Cu, Fe and Mn.

The gamma-ray transmission method has been reported as the most accurate and convenient technique for non-destructive measurements of soil parameters, including the linear attenuation coefficient, field capacity, moisture content, bulk density and porosity [1]. In laboratory experiments, lead is used for shielding purposes. In field conditions, soil may be used as a radiation shielding material. The use of soil as the shielding is advantageous from the perspectives of cost and availability [2]. To interpret the behavior and performance of soils as radiation shielding materials, it is important to identify soil photon energy absorption parameters, such as the mass attenuation coefficients (μ_s), the effective atomic numbers (Z_{eff}) and the effective electron densities (N_{eff}).

The photon attenuation coefficient is an important parameter that characterizes the penetration and diffusion of gamma-rays in composite materials such as soils [3]. This coefficient is a measure of the average number of interactions that occur between gamma-rays and the matter mass per unit area. The μ_s depends on the chemical composition of the absorbing material and the incident photon energy. However, for the total photon interaction, the variation of μ_s with the soil composition is large below 50 keV, and negligible above 300 keV, up to 3 MeV [4]. Studies of Z_{eff} provide conclusive information about the target related to the radiation interactions [5]. A commonly used method to determine the Z_{eff} value for a composite material is based on the determination of the μ_s values for gamma-ray interactions using the transmission method. Z_{eff} represents the interaction of radiation with the matter being studied, and is a convenient parameter to consider when designing radiation shields and computing the absorbed dose, energy absorption and exposure build-up factors. The Z_{eff} and N_{eff} values vary with energy, depending on the interaction processes involved. The energy absorption in a given medium can be calculated if certain constants are known. These necessary constants are the Z_{eff} and N_{eff} values of the medium. Consequently, these constants have been defined and computed in many different ways by various researchers [6–42]. However, only a limited amount of work has been reported in the literature on the photon energy absorption parameters for different soil samples [43–55]. Therefore, this work concentrates on the theoretical and experimental determination of the photon energy absorption parameters of different soils. Photon energy absorption parameters (i.e. μ_s, Z_{eff} and N_{eff}) were calculated for photon energies in the range 1 keV–15 MeV, and the results were compared with the measurements obtained with photon energies of 661.6, 1173.2 and 1332.5 keV for five different soil samples, i.e. Soils 1, 2, 3, 4 and 5. The soils under consideration were collected from Bursa (Turkey). The gamma-ray attenuation measurements were performed using ^{137}Cs and ^{60}Co radioactive sources.

MATERIALS AND METHODS

Theory

When a gamma-ray beam passes through a soil sample of thickness x (cm), the photons are transmitted according to Beer–Lambert's law [56]. This process is expressed as follows:

$$I = I_0\ exp(-\mu x), \qquad (1)$$

where I_0 is the initial intensity of the gamma-rays, I is intensity of the gamma-rays after attenuation through a soil column of length x, and μ (cm^{-1}) is the linear attenuation coefficient of the dry soil. The linear attenuation coefficient can be described as follows:

$$\mu = (\mu/\rho)\rho, \qquad (2)$$

where $\mu_s = \mu/\rho$ (cm^2/g) is the mass attenuation coefficient and ρ is the density of the soil sample. Equation (1) can be rewritten as follows:

$$I = I_0\ exp(-\mu_s d) \qquad (3)$$

where d (g/cm^2) is the mass thickness of the dry soil sample. Equation (3) may be written in the following linear form:

$$\ln I = -\mu_s d + \ln I_0 \qquad (4)$$

μ_s can be obtained from the measured values of (I/I_0) and d. The total μ_s values for materials composed of multiple elements are the sums of the $(\mu_s)_i$ values of each constituent element according to the following mixture rule [57]:

$$\mu_s = \sum_i W_i(\mu_s)_i, \qquad (5)$$

where W_i is the fractional atomic mass of the elements and $(\mu_s)_i$ is the mass attenuation coefficient of the ith element in the mixture. For materials composed of multiple elements, the fraction by atomic mass is given by

$$W_i = n_i A_i / \left[\sum_j n_j A_j\right], \qquad (6)$$

where A_i is the atomic weight of the ith element and n_i is the number of formula units. The total atomic cross-sections (σ_t) for the sample can be obtained from the measured values of μ_s using the following relation [58]:

$$\sigma_t = (1/N_A)\left[\mu_s / \left(\sum_i \frac{W_i}{A_i}\right)\right], \qquad (7)$$

where N_A is Avogadro's number. The total electric cross-section (σ_e) is given by the following formula [22]:

$$\sigma_e = (1/N_A)\left[\sum_i (f_i A_i / Z_i)(\mu_s)_i\right] = \sigma_t / Z_{eff}, \qquad (8)$$

where f_i is the number fraction of the atoms of element i relative to the total number of the atoms of all elements in the mixture, and Z_i is the atomic number of the ith elements in the mixture. σ_t and σ_e are related to the Z_{eff} of the material through the following expression [22]:

$$Z_{eff} = \sigma_t / \sigma_e \qquad (9)$$

The N_{eff} (number of electrons per unit mass) can be written as following:

$$N_{eff} = (N_A/A_i)(Z_{eff}) \sum_i n_i = \mu_s / \sigma_e \qquad (10)$$

The μ_s values of the materials have been calculated using the WinXCom program [59]. This well-known and widely used program provides the total mass attenuation coefficient and total attenuation cross-section data for approximately 100 elements, as well as the partial cross-sections for incoherent and coherent scattering, photoelectric absorption and pair production at energies from 1 keV to 100 GeV [59]. All computations in the present work have been performed using the WinXCom program.

Experimental details

The soil samples used in this study were taken from a soil tillage depth. The soils were classified as Entisol (Soil 1, Soil 2, and Soil 5), Inceptisol (Soil 3) and Alfisol (Soil 4), according to the Soil Taxonomy [60]. According to the results of the soil analysis, the soils were primarily medium-textured, had neutral or slightly alkaline pHs, contained different amounts of lime, and primarily had a low organic matter content. There was no salinity problem in the soils. The soil samples considered were analyzed for the percentage of clay, silt and sand using the hydrometer method [61]. Some physical characteristics of the soils, along with their sample codes, are presented in Table 1.

The soil samples were passed through a 2-mm sieve. Each soil was then dried in a 105°C oven for 24 h and packed in a Perspex box. The chemical composition of the soil samples were analyzed using an energy-dispersive X-ray fluorescence (EDXRF) spectrometer from SPECTRO (X-LAB 2000), which had a 400 W Pd end-window X-ray tube, sample trays for 32 mm (20 positions) and 40 mm (12 positions) samples, 47 mm Teflon filters, and an N_2-cooled Si (Li) detector with the required electronics (i.e. amplifier, ADC and multichannel analyzer). The EDXRF analyses (major-element compositions and trace-element analyses) were performed in the Bursa Test and Analysis Laboratory (BUTAL). The chemical compositions of these soil samples are given in Table 2. The soil samples studied have different chemical composition and different fractions (i.e. sand, silt and clay).

The schematic arrangement of the experimental set-up used in the present study is shown in Fig. 1. The soil samples were kept in a polyethylene box that was 6.5 cm high and 11 cm in diameter. The point sources were placed on the symmetry axis of the polyethylene box and over the soil level. The samples were separately irradiated with ^{137}Cs (661.6 keV) and ^{60}Co (1173.2 and 1332.5 keV) radioactive point sources. Each source had an activity of 10 μCi (370 kBq). The pulse-height spectra of the gamma-rays transmitted through the soil were measured using a 2″ × 2″ cylindrical NaI(Tl) detector connected to the Canberra Series 40 Multi-Channel Analyzer (MCA) system with 2048 channels. The detector was positioned on the symmetry axis of the box. The detector assembly was surrounded by lead shielding. Both the soil sample and the point source were also surrounded by lead collimators inside the lead castle.

The measurements for all samples were taken to have good statistics and performed three times for each energy value to improve the statistical error. The transmitted spectra were recorded with the MCA for a time period that was sufficient to obtain the desired precision and accuracy of the results. The peak areas were calculated from the

Table 1. Some physical characteristics of the soils

Soil code	Geographic coordinate of the soils		Soil type	Particle size distribution (%)				
	X(East)	Y (North)		Sand	Silt	Clay	TC	ρ (g/cm^3)
Soil 1	599956	4449947	Entisol	35.3	42.0	22.7	L	1.38
Soil 2	598362	4451236	Entisol	58.6	22.0	19.4	SL	1.45
Soil 3	698495	4491031	Inceptisol	59.1	18.0	22.9	SCL	1.42
Soil 4	651463	4449239	Alfisol	29.3	18.0	52.7	C	1.24
Soil 5	633706	4425913	Entisol	30.0	42.0	28.0	CL	1.34

TC = Soil Texture Class, L = Loam, SL = Sandy Loam, SCL = Sandy Clay Loam, C = Clay, CL = Clay Loam. (The texture classes are based on USDA classification).

Table 2. EDXRF analysis results of the dry soil samples

Soil code	Chemical components (%)											
	Na_2O	MgO	Al_2O_3	SiO_2	P_2O_5	K_2O	CaO	TiO_2	Cr_2O_3	MnO	Fe_2O_3	LOI
Soil 1	1.39	2.442	14.62	63	0.170 3	2.79	6.78	0.595 1	0.017 81	0.073 3	4.312	3.6
Soil 2	2.02	1.3	12.75	78.4	0.321 05	2.51	1.76	0.503 1	0.010 97	0.073 535	2.79	<1
Soil 3	2.45	1.04	16.1	68.3	0.125 85	1.644	3.89	0.638 6	0.007 3	0.109 55	5.791	<1
Soil 4	0.230 5	1.94	13.14	55.9	0.112 55	1.91	11	0.599 55	0.027 095	0.096 44	4.53	10
Soil 5	0.11	9	10.66	39.62	0.221 4	0.379 45	15.9	0.413 1	0.037 78	0.053 13	4.38	19.2

LOI = Loss of Ignition

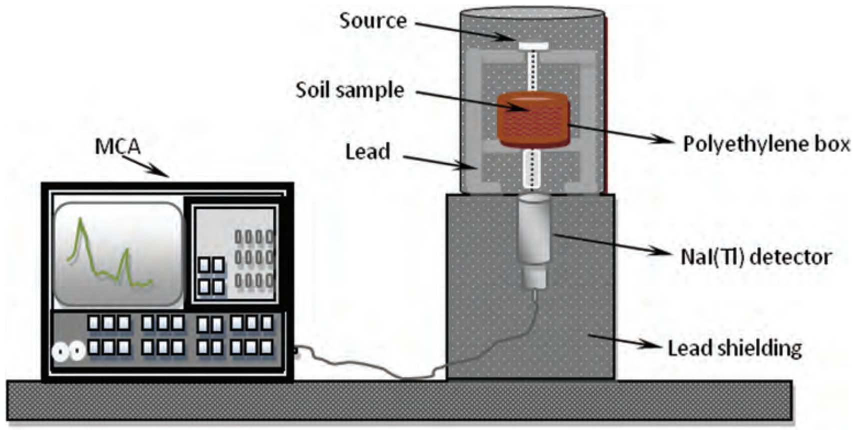

Fig. 1. The schematic arrangement of the experimental setup.

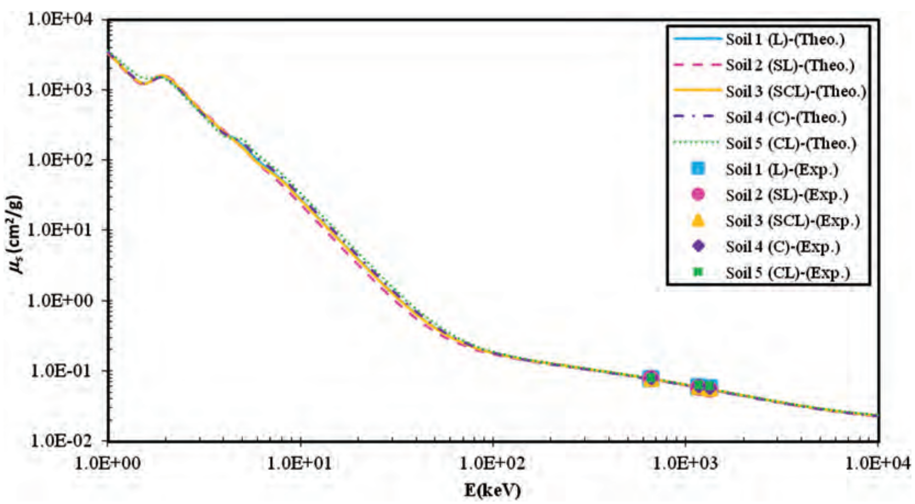

Fig. 2. The calculated mass attenuation coefficients of the soil samples within the 1 keV–15 MeV photon energy range and a comparison between measurements and photon energies.

spectra obtained for each measurement. The μ_s values of the soils were calculated from Equation (4) for known physical densities using the gamma transmission measurements for the dry soil samples.

The maximum errors in the total mass attenuation coefficients were calculated from the errors in the intensities I_0 (without sample) and I (with sample) and the errors in the physical densities, using the following relation:

$$\Delta\mu_s = \frac{1}{\rho x}\sqrt{\left(\frac{\Delta I_0}{I_0}\right)^2+\left(\frac{\Delta I}{I}\right)^2+\left[ln\left(\frac{I_0}{I}\right)\right]^2\left[\left(\frac{\Delta\rho}{\rho}\right)^2+\left(\frac{\Delta x}{x}\right)^2\right]}, \quad (11)$$

where χ is the sample thickness in centimeters, ΔI_0, ΔI and $\Delta\rho$ are the errors in the intensities I_0 and I and the density ρ, respectively. In these experiments, the net counts I_0 and I were obtained for the same amount of time and under the same experimental conditions. The overall uncertainty ithe experimental measurements was < 3%. This uncertainty is mainly due to the counting statistics, the thickness measurements, the evaluation of the peak areas, and the scattered photons reaching the detector.

RESULTS AND DISCUSSION

The μ_s values for the different soil samples were also calculated for photon energies in the range of 1 keV–15 MeV. The results were plotted versus the photon energy with the measurement values for energies of 661.6, 1173.2 and 1332.5 keV in Fig. 2. The experimental and theoretical results are clearly in good agreement for all of the studied soil samples. Figure 2 shows that the μ_s values are large and show a decreasing trend, with strong energy dependence in the low incident photon energy range of 1–100 keV. In the intermediate (100 keV–1 MeV) and high (1–15 MeV) energy regions, the μ_s values show a less energy-dependent behavior and gradually decrease with the increasing incident photon energy. Fig. 3 shows the incident photon energy dependence of the measured μ_s values for all of the studied soils.

Note that μ_s depends on the incoming photon energies because the partial photon-matter interactions (such as photoelectric absorption, Compton scattering and pair production) in the nuclear and electric fields are different for different photon energies. Due to the dominant photoelectric absorption, the μ_s values show a strong incident photon energy dependence in the low energy range because μ_s is inversely proportional ($1/E^{3.5}$ dependence) to the incident energy. The differences observed in the μ_s values for the soils in the low energy region can be attributed to the dominance of photoelectric absorption because the photoelectric cross-section is strongly dependent (Z^4 or Z^5 dependence) on the atomic number of the constituent elements [16, 62].

Compton (inelastic) scattering starts to dominate over the photoelectric absorption process when the incident photon energy exceeds ~100 keV, up to ~1 MeV. In this intermediate energy range, no significant differences in the behavior of the different soils are observed because the composition effects play a less significant role in Compton scattering (linear Z dependence) relative to photoelectric absorption.

In the high energy region, the pair production processes in the nuclear and electric fields come into prominence after certain thresholds above 1 MeV are exceeded. The energy dependence of μ_s thus changes its slope relative to the intermediate energy region.

The Z_{eff} values for all soil samples have been calculated using Equation (9) for photon energies in the range of 1 keV–15 MeV in 36 energy steps. The results have been plotted against the photon energies, as shown in Fig. 4. In this figure, the theoretical results were also compared with the experimental results performed with photon energies of 661.6, 1173.2 and 1332.5 keV. A good agreement between the theoretical and measurement results has clearly been obtained. The Z_{eff} values of the soil samples change with a change in the energy. However, the behavior of Z_{eff} with respect to the energy is rather interesting. The Z_{eff} values for all of the soil samples show a small decrease with increasing energy in the range of 1–1.5 keV and a sharp increase with increasing energy in the range of 1.5–2 keV. The Z_{eff} values then sharply decrease again with increasing energy up to 8 keV (up to 10 keV for Soils 2 and 4). The Z_{eff} values are nearly constant between 8 and 40 keV photon energies (in the energy region of 10–30 keV for Soils 2 and 4). Beyond this energy region, the Z_{eff} values increase again with increasing energy in the range of 40–300 keV. The Z_{eff} values are then nearly constant again in the energy region of 300 keV–5 MeV and decrease again with increasing energy, up to 15 MeV. This decrease in the Z_{eff} values is small but continuous.

This significant variation in the Z_{eff} values for all of the soil samples is because of the relative domination of the partial photon interaction mechanism (e.g. photoelectric absorption, Compton scattering and pair production). This variation also depends on the range of the atomic numbers of soil constituent elements and the number of elements in the composite material. The atomic numbers of the elements of the selected soils vary from 8 (O_2) to 26 (Fe), and a total of 12 elements are considered. As expected, the Z_{eff} values of the soils lie within the range of the atomic numbers of their constituent elements ($8 < Z_{eff} < 26$).

The N_{eff} values for all of the soil samples have been calculated using Equation (10) for photon energies in the range of 1 keV–15 MeV in 36 energy steps. The results have been plotted against photon energies, as shown in Fig. 5. In this figure, the theoretical results were also compared with the experimental results obtained with photon

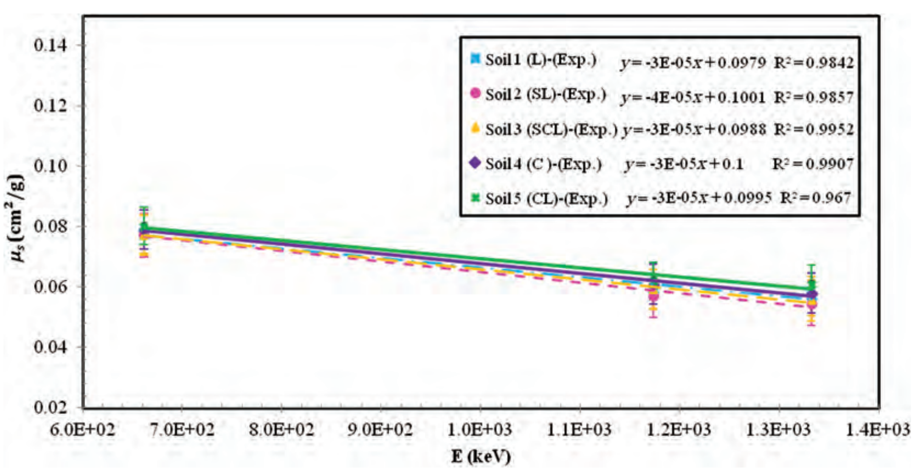

Fig. 3. Measured mass attenuation coefficients of the soil samples at 661.6, 1173.2 and 1332.5 keV.

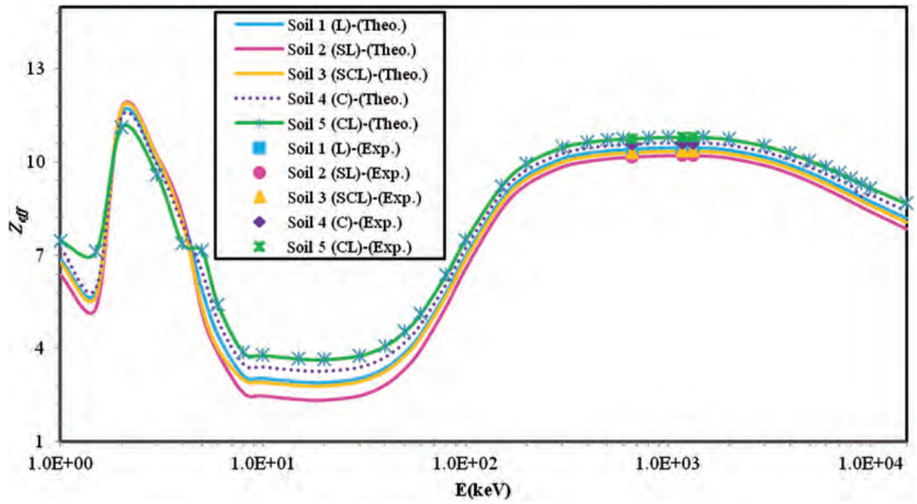

Fig. 4. The effective atomic number of the soil samples as a function of photon energy.

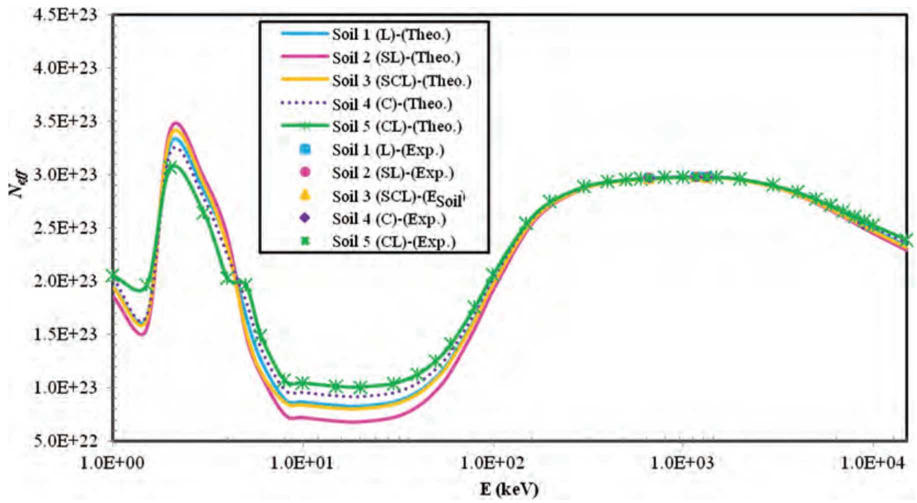

Fig. 5. The effective electron density of the soil samples as a function of photon energy.

energies of 661.6, 1173.2 and 1332.5 keV. There are slight differences in the N_{eff} values for different soils, where a higher value of the electron density would indicate an increased probability of a photon-electron energy transfer and an energy deposition into the material. The N_{eff} values show a photon–energy dependence similar to that observed for Z_{eff}. This is confirmed in Fig. 6, which shows the correlation of the Z_{eff} and N_{eff} values obtained from the theoretical calculation and experimental results.

Different proportions of sand, silt and clay give rise to the different types of loam soils: loam (L), sandy loam (SL), sandy clay loam (SCL), clay (C), clay loam (CL), silt loam and silt clay loam. Sandy loam, due to the larger size of its particles, feels gritty. Clay loam, due to the smaller size of its particles, feels sticky. Silt loam, being moderate in size, has a smooth or floury texture. From Table 1, it can be observed that Soils 1, 2, 3, 4 and 5 have the texture classes of L, SL, SCL, C and CL, respectively. Soils 2 (SL) and 3 (SCL) demonstrate poor photon energy absorption characteristics (i.e. low μ_s, Z_{eff} and N_{eff}). However, Soils 5 (CL) and 4 (C) soils have good photon energy absorption characteristics (i.e. high μ_s, Z_{eff} and N_{eff}). These results may be due to the compositional variation among the different types of the soils and the effects of the soil grain size on the gamma-ray attenuation. Furthermore, it can be observed from Table 2 that Soil 5 (CL) has the minimum percentage of SiO_2 (39.62%) and the maximum contribution of CaO (15.9%), whereas Soil 2 (SL) has the minimum amount of CaO (1.76%) and the maximum percentage of SiO_2 (78.4%). The photon energy-absorption parameters of the

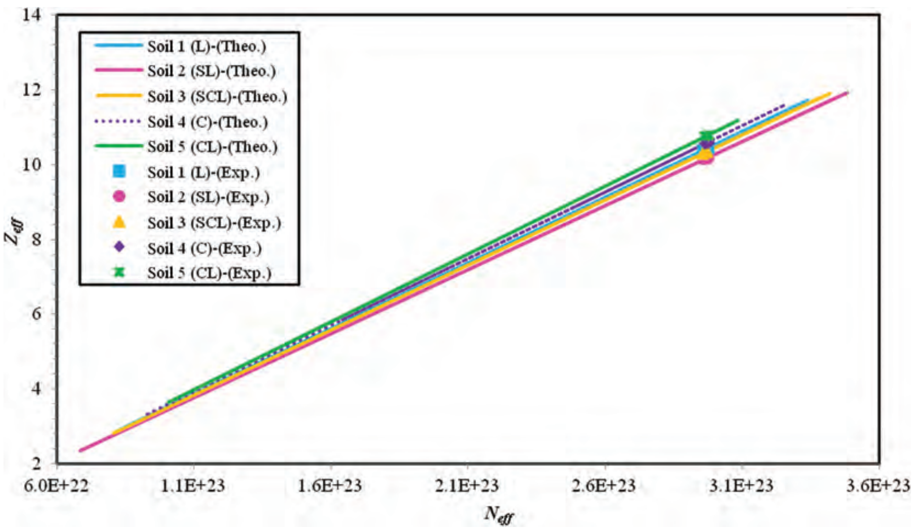

Fig. 6. Correlation between the effective atomic number and the electron density of the soils for the theoretical and experimental results.

clay loam are higher where the CaO weight percentage is greater and that of SiO_2 is smaller. The photon energy absorption parameters of sandy loam are also lower where the SiO_2 weight percentage is greater and that of CaO is smaller.

CONCLUSION

It can be concluded from this work that the photon energy-absorption parameters depend on the photon energies and the chemical composition of the soil samples. A good agreement was observed between the theoretical calculations and experimental results. The dependence of μ_s on both the photon energy and soil composition is remarkable in the low incident energy range due to the dominant photoelectric absorption mechanism. The compositional effects and photon energy dependencies are reduced from the intermediate energy range to the high energy range because Compton scattering and pair production processes start to dominate the photon absorption process.

Among the investigated soil samples, the photon absorption effectively increases in the following order: Soil 5 (clay loam) > Soil 4 (clay) > Soil 1 (loam) > Soil 3 (sandy clay loam) > Soil 2 (sandy loam). The sandy loam and sandy clay loam soils demonstrate poor photon energy absorption characteristics (i.e. low μ_s, Z_{eff} and N_{eff}). However, the clay loam and clay soils have good photon energy absorption characteristics (i.e. high μ_s, Z_{eff} and N_{eff}).

ACKNOWLEDGEMENTS

This work was supported by the Commission of Scientific Research Projects of Uludag University, Project Number UAP(F)-2011/74. We are thankful to the Bursa Test and Analysis Laboratory (BUTAL) and Dr M. Akif Cimenoglu for the EDXRF analysis.

FUNDING

This work was supported by the Commission of Scientific Research Projects of Uludag University, Project Number UAP(F)-2011/74.

REFERENCES

1. Mudahar GS, Sahota HS. A new method for simultaneous measurement of soil bulk density and water content. *Int J Appl Radiat Isot* 1986;**37**:563.
2. Brar GS, Sidhu GS, Sandhu PS *et al*. Variation of buildup factors of soils with weight fractions of iron and silicon. *Appl Radiat Isot* 1998;**49**:977–80.
3. Singh M, Mudahar S. Energy dependence of total photon attenuation coefficients of composite materials. *Appl Radiat Isot* 1992;**43**:907–11.
4. Mudahar GS, Modi S, Singh M. Total and partial mass attenuation coefficients of soil as a function of chemical composition. *Appl Radiat Isot* 1991;**42**:13–8.
5. Singh K, Kaur R, Vandana *et al*. Study of effective atomic numbers and mass attenuation coefficients in some compounds. *Radiat Phys Chem* 1996;**47**:535–41.
6. Hine GJ. The effective atomic numbers of materials for various gamma interactions. *Phys Rev* 1952;**85**:725.
7. Henriksen T, Baarli J. The effective atomic number. *Radiat Res* 1957;**6**:415–23.
8. Murty RC. Effective atomic numbers of heterogeneous materials. *Nature* 1965;**207**:398–9.

9. Parthasaradhi K. Studies on the effective numbers in the alloy for gamma ray interactions in the energy region 100-662 keV. *Indian J Pure Appl Phys* 1968;**6**:609–13.
10. Jayachandran CA. Calculated effective atomic number and Kerma values for tissue equivalent and dosimetry materials. *Phys Med Biol* 1971;**16**:617–23.
11. White DR. An analysis of the Z-dependence of photon and electron interactions. *Phys Med Biol* 1977;**22**:219–28.
12. Manninen S, Koikkalainen S. Determination of the effective atomic number using elastic and inelastic scattering of γ–rays. *Appl Radiat Isot* 1984;**35**:965–8.
13. Yang NC, Leichner PK, Hawkins WG. Effective atomic number for low-energy total photon interactions in human tissues. *Med Phys* 1987;**14**:759–66.
14. El-Kateb AH, Abdul-Hamid AS. Photon attenuation coefficient study of some materials containing hydrogen, carbon and oxygen. *Appl Radiat Isot* 1991;**42**:303–7.
15. Bhandal GS, Ahmed I, Singh K. Determination of effective atomic number and electron density of some fatty acids by gamma-ray attenuation. *Appl Radiat Isot* 1992;**43**:1185–8.
16. Bhandal GS, Singh K. Photon attenuation coefficient and effective atomic number study of cements. *Appl Radiat Isot* 1993;**44**:1231–43.
17. Kumar TK, Reddy KV. Effective atomic numbers for materials of dosimetric interest. *Radiat Phys Chem* 1997;**50**:545–53.
18. Gill H, Kaur G, Singh K *et al*. Study of effective atomic numbers in some glasses and rocks. *Radiat Phys Chem* 1998;**51**:671–2.
19. Koç N, Özyol H. Z-dependence of partial and total photon interactions in some biological samples. *Radiat Phys Chem* 2000;**59**:339–45.
20. Nayak NG, Vijaya MG, Siddappa K. Effective atomic numbers of some polymers and other materials for photoelectric process at 59.54 keV. *Radiat Phys Chem* 2001;**61**:559–61.
21. Shivaramu, Vijayakumar R, Rajasekaran L *et al*. Effective atomic numbers for photon energy absorption of some low-Z substances of dosimetric interest. *Radiat Phys Chem* 2001;**62**:371–7.
22. Singh K, Singh H, Sharma V *et al*. Gamma-ray attenuation coefficients in bismuth borate glasses. *Nucl Instrum Meth B* 2002;**194**:1–6.
23. Shakhreet BZ, Chong CS, Bandyopadhyay T *et al*. Measurement of photon mass–energy absorption coefficients of paraffin wax and gypsum at 662 keV. *Radiat Phys Chem* 2003;**68**:757–64.
24. İçelli O, Erzeneoğlu S. Effective atomic numbers of some vanadium and nickel compounds for total photon interactions using transmission experiments. *J Quant Spectrosc Ra* 2004;**85**:115–24.
25. Akkurt I, Mavi B, Akkurt A *et al*. Study on Z dependence of partial and total mass attenuation coefficients. *J Quant Spectrosc Ra* 2005;**94**:379–85.
26. Manjunathaguru V, Umesh TK. Effective atomic numbers and electron densities of some biologically important compounds containing H, C, N and O in the energy range 145-1330 keV. *J Phys B At Mol Opt Phys* 2006;**39**:3969–81.
27. Akar A, Baltaş H, Çevik U *et al*. Measurement of attenuation coefficients for bone, muscle, fat and water at 140, 364 and 662 keV γ-ray energies. *J Quant Spectrosc Ra* 2006;**102**:203–11.
28. Manohara SR, Hanagodimath SM. Studies on effective atomic numbers and electron densities of essential amino acids in the energy range 1 keV–100 GeV. *Nucl Instrum Meth B* 2007;**258**:321–8.
29. Singh MP, Sandhu BS, Singh B. Measurement of effective atomic number of composite materials using scattering of γ-rays. *Nucl Instrum Meth A* 2007;**580**:50–3.
30. Kaliman Z, Orlić N, Jelovica I. Calculations of effective atomic number. *Nucl Instrum Meth A* 2007;**580**:40–2.
31. Suresh KC, Manjunatha HC, Rudraswamy B. Study of Z_{eff} for DNA, RNA and RETINA by numerical methods. *Radiat Prot Dosim* 2008;**128**:294–8.
32. İçelli O, Erzeneoğlu S, Sağlam M. Effective atomic numbers of polypyrrole via transmission method in the energy range 15. 74–40.93 keV. *Ann Nucl Energy* 2008;**35**:432–7.
33. Demir L, Han I. Mass attenuation coefficients, effective atomic numbers and electron densities of undoped and differently doped GaAs and InP crystals. *Ann Nucl Energy* 2009;**36**:869–73.
34. Özdemir Y, Kurudirek M. A study of total mass attenuation coefficients, effective atomic numbers and electron densities for various organic and inorganic compounds at 59.54 keV. *Ann Nucl Energy* 2009;**36**:1769–73.
35. Manohara SR, Hanagodimath SM, Thind KS *et al*. The effective atomic number revisited in the light of modern photon-interaction cross-section databases. *Appl Radiat Isot* 2010;**68**:784–7.
36. Baştuğ A, Gürol A, İçelli O *et al*. Effective atomic numbers of some composite mixtures including borax. *Ann Nucl Energy* 2010;**37**:927–33.
37. Medhat ME. Studies on effective atomic numbers and electron densities in different solid state track detectors in the energy range 1 keV–100 GeV. *Ann Nucl Energy* 2011;**38**:1252–63.
38. Baştuğ A, İçelli O, Gürol A *et al*. Photon energy absorption parameters for composite mixtures with boron compounds. *Ann Nucl Energy* 2011;**38**:2283–90.
39. Damla N, Baltas H, Celik A *et al*. Calculation of radiation attenuation coefficients, effective atomic numbers and electron densities for some building materials. *Radiat Prot Dosim* 2011;**28**:1–9.
40. Kurudirek M. Estimation of effective atomic numbers of some solutions for photon energy absorption in the energy region 0.p2–1.5 MeV: An alternative method. *Nucl Instrum Meth A* 2011;**659**:302–6.
41. Han I, Aygun M, Demir L *et al*. Determination of effective atomic numbers for 3d transition metal alloys with a new semi-empirical approach. *Ann Nucl Energy* 2012;**39**:56–61.
42. Chanthima N, Kaewkhao J, Limsuwan P. The parameters of photon energy absorption for silicate glasses containing with BaO, PbO and Bi_2O_3. *Procedia Eng* 2012;**32**:833–8.

43. Mudahar GS, Sahota HS. Effective atomic number studies in different soils for total photon interaction in the energy region 10-5000 keV. *Appl Radiat Isot* 1988;**39**:1251–4.
44. Oliveira JCM, Appoloni CR, Coimbra MM *et al*. Soil structure evaluated by gamma-ray attenuation. *Soil Till Res* 1998;**48**:127–33.
45. Elias EA, Bacchi OOS, Reichardt K. Alternative soil particle-size analysis by gamma-ray attenuation. *Soil Till Res* 1999;**52**:121–3.
46. Akbal S, Baytas AF. Determination of the photon attenuation coefficients for Turkish soils by gamma transmission. *Bulg J Phys* 2000;**27**:1–4.
47. Alam MN, Miah MMH, Chowdhury MI *et al*. Attenuation coefficients of soils and some building materials of Bangladesh in the energy range 276-1332 keV. *Appl Radiat Isot* 2001;**54**:973–6.
48. Baytaş AF, Akbal S. Determination of soil parameters by gamma-ray transmission. *Radiat Meas* 2002;**35**:17–21.
49. Elias EA. A simplified analytical procedure for soil particle-size analysis by gamma-ray attenuation. *Comput Electron Agr* 2004;**42**:181–4.
50. Pires LF, Bacchi OOS, Reichardt K. Soil water retention curve determined by gamma-ray beam attenuation. *Soil Till Res* 2005;**82**:89–97.
51. Demir D, Ün A, Özgül M *et al*. Determination of photon attenuation coefficient, porosity and field capacity of soil by gamma-ray transmission for 60, 356 and 662 keV gamma rays. *Appl Radiat Isot* 2008;**66**:1834–7.
52. Groot AV, Graaf ER, Meijer RJ *et al*. Sensitivity of *in-situ* γ-ray spectra to soil density and water content. *Nucl Instrum Meth A* 2009;**600**:519–23.
53. Raje DV, Chaudhari LM. Mass attenuation coefficients of soil samples in Maharashtra State (India) by using gamma energy at 0.662 MeV. *Bulg J Phys* 2010;**37**:158–64.
54. Ün A, Demir D, Şahin Y. Determination of density and volumetric water content of soil at multiple photon energies. *Radiat Phys Chem* 2011;**80**:863–8.
55. Medhat ME. Application of gamma-ray transmission method for study the properties of cultivated soil. *Ann Nucl Energy* 2012;**40**:53–9.
56. Wang CH, Willis DL, Loveland WD. Characteristics of ionizing radiation. In: Wang CH, Willis DL, Loveland WD (eds). *Radiotracer Methodology in the Biological, Environmental and Physics Sciences*, Englewood Cliffs, NJ: Prentice-Hall, 1975, pp. 39–74.
57. Hubbell JH, Seltzer SM. Tables of X-ray mass attenuation coefficients and mass energy-absorption coefficients 1 keV-20 MeV for elements Z=1 to 92 and 48 additional substances of dosimetric interest. National Institute of Standarts and Physics Laboratory NISTIR 1995, 5632.
58. Wang DC, Ping LA, Yang H. Measurement of the mass attenuation coefficients for SiH_4 and Si. *Nucl Instrum Meth B* 1995;**95**:161–5.
59. Gerward L, Guilbert N, Jensen KB *et al*. WinXCom–a program for calculating X-ray attenuation coefficients. *Radiat Phys Chem* 2004;**71**:653–4.
60. USDA NRCS [United States Department of Agriculture Natural Resources Conservation Service]. *Soil Taxonomy: A basic system of soil classification for making and interpreting soil surveys,* 2nd edn, Agriculture Handbook Number: 436. Washington, DC: Government Printing Office, 1999, 863.
61. Gee GW, Bauder JW. Particle size analysis. In: Klute A (ed). *Methods of Soil Analysis. Part 1.* 2nd edn. Madison, WI: Argon. Monogr. 9. ASA, 1986, pp. 383–411.
62. Singh T, Rajni, Kaur U *et al*. Photon energy absorption parameters for some polymers. *Ann Nucl Energy* 2010;**37**:422–7.